Phytoplankton Studies in the South Shetland Islands

Christopher D. Hewes, Osmund Holm-Hansen, José Luis Iriarte, Nicolas Sanchez Puerto, Douglas Krause, and Nelson Silva

Abstract Hydrographic, chemical, and biological data relevant to phytoplankton productivity in the South Shetland Islands region were collected in January and Febrary of 2009. According to the 2008/09 AMLR Survey:

- A total of 104 phytoplankton samples were taken at stations on the AMLR Survey grid.
- Mean Chl-*a* concentrations in the Upper Mixed Layer (UML) were lowest in the Elephant Island (~0.7 mg m^{-3}) and West (~0.4 mg m^{-3}) Areas, but comparable to the historical mean. Highest mean Chl-*a* concentrations were measured in the Joinville Island Area and the South Area.
- Two stations in the Joinville Island Area had unexpectedly high Chl-*a* concentrations. This area might need further investigation to understand .

Introduction

The ability to ultimately manage various trophic groups in the Antarctic, as envisioned by CCAMLR, must be based on a thorough understanding of food web dynamics, including the food resources available to Antarctic krill and other zooplankton in the region. It is thus important to develop a better understanding of the distribution of phytoplankton (the primary producers) at seasonal and inter-annual scales.

Our research component is primarily concerned with documenting the magnitude and quality of food available to zooplankton, and with improving our understanding of the relationships between the physical, chemical and optical water properties, which determine the amount of food available throughout the summer season. Here, we give preliminary results from the 2009 field season of the AMLR Survey. We also refine our understanding of these relationships in the South Shetland Islands with respect to biomass and productivity of phytoplankton.

Methods

Water column data were obtained from a conductivity-temperature-depth (CTD) sensor carousel, which held the water sampling bottles and a number of other instruments and sensors. The carousel was lowered to 750 m depth or to within 10 m of the bottom at the shallower stations. The bottles were closed on the up-cast at 5, 30, 50, 75, and 100 m target depths for Chl-*a* analyses. At the time of bottle closure, a ~1 second binned record was obtained of all data recorded by sensors on the carousel. Additionally, 24 samples from 30 m depth were (1) preserved for floristic analyses and (2) frozen for nutrient analyses.

A complete list of instruments on the CTD can be found in the Physical Oceanography section in this report (Needham, 2009). In addition to CTD instrumentation, a LI-COR Quantum Sensor (LI-190) was mounted in a shade-free area above the bridge to measure (1 minute intervals) incident photosynthetically available radiation (PAR) (see Physical Oceanography report for details).

Sensor Calibrations and Internal Correlations

The Chelsea Aqua^{tracka} III fluorometer mounted on the CTD carousel has a log voltage output. This was converted to a linear Chl-*a* concentration equivalent by exponential regression (Figure 2.1) of extracted Chl-a concentration and fluorometer voltage obtained during CTD bottle firing for samples obtained in the Upper Mixed Layer (UML) (n = 254, $r^2 = 0.68$) as:

$$\text{mg Chl}_{\text{fluor}}\ \text{m}^{-3} = 0.0168 \bullet \exp(2.3791 \bullet \text{Volts}).$$

Measurements and Data Acquired

The types of measurements and the data acquired during the 2009 AMLR Survey were:

(A) Chlorophyll-*a* concentrations: Chl-*a* concentrations of water samples were determined by measurement of

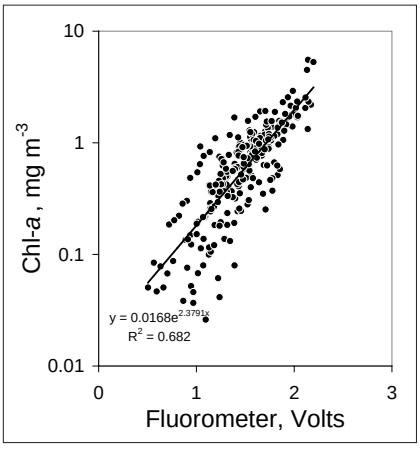

Figure 2.1. Chelsea Aqua^{tracka} III calibration. Concentrations of Chl-*a* determined from water bottle samples obtained within the UML plotted against fluorometer voltage obtained at the time of water bottle firing. The fluorometer has a log voltage output with respect to Chl-*a* concentration. The equation (and r^2) is the exponential function used to provide equivalent Chl-a concentrations (Chl_{fluor}) as derived from the fluorometer. Line is the exponential regression for the relationship.

Chl-*a* fluorescence after extraction in an organic solvent. Water samples (100 mL; for routine measurements) were filtered through glass fiber filters (Whatman GF/F, 25 mm) at reduced pressure (maximal differential pressure of 1/3rd atmosphere). The remaining particulate material was placed in 10 mL of absolute methanol, in 15 mL tubes, at 4 °C for at least 12 hours to extract the photosynthetic pigments from the filter. The samples were then shaken, centrifuged, and the clear supernatant poured into cuvettes (13 x 100 mm) for measurement of Chl-*a* fluorescence before and after the addition of two drops of 1.0 N HCl (Holm-Hansen et al., 1965; Holm-Hansen and Riemann, 1978). Fluorescence was measured using a Turner Designs Fluorometer (TD-700) that had been calibrated using purified Chl-*a* concentrations (Sigma C-6144).

(B) Continuous profiles of Chl-*a* and PAR: Profiles of Chl-*a* obtained with the *in situ* fluorometer were used to analyze Chl-*a* concentration in relation to physical, chemical, and optical conditions in the water column.

(C) Beam attenuation (C_p): The attenuation of light, as recorded by the transmissometer, is the result of both scattering and absorption of light quanta. As the light in the transmissometer that was used is 660 nmi (within the red absorption band for Chl-*a*), the attenuation is a good indicator of both Chl-*a* concentrations and total particulate organic carbon (Villafañe et al., 1993).

Transmission of light though water with the near-absence of particulate matter was obtained from the mean of all transmissometer voltages (V_0) from CTD casts in pelagic waters (bottom depth > 2000 m) measured at depths 700-750 m. The transmissometer has a path-length of 0.25 m and has a linear output in Volts, thus C_p was estimated as:

$$C_p \text{ (meters}^{-1}) = -\ln(\text{Transmittance}),$$

and

$$\text{Transmittance} = [(V_0 - \text{Volts}) / V_0] / 0.25 \text{ m}.$$

(D) Phytoplankton taxonomy: Seawater samples (100 mL) were obtained within the upper mixed layer and preserved with 0.5% (final dilution) buffered formalin at 24 stations. These samples were delivered to J. L. Iriarte (Universidad Austral de Chile, Puerto Montt, Chile) for taxonomic analysis of phytoplankton species.

(E) Inorganic macronutrient concentrations: Water samples were taken for measurement of macronutrient concentrations at 30 m for 22 stations, plus two stations in the Drake Passage at 10, 30, 50, 75, and 100 m target depths, poured into acid-washed 120 mL polypropylene bottles, and immediately frozen. All frozen samples were delivered to N. Silva (Universidad Católica de Valparaiso, Valparaiso, Chile) and analyzed by auto-analyzer for nitrate, phosphate, and silicate concentrations (Atlas et al., 1971).

(F) UML depth (Z_{UML}): Depth of the UML was calculated as the depth at which potential density differed by 0.05 kg m^{-3} from the mean potential density measured between 5 and 10 m depth (Mitchell and Holm-Hansen, 1991; Hewes et al., 2008a). Values representing the UML were obtained by averaging all samples taken above the UML depth (1 m binned data for sensor data and individual bottle data for Chl-*a*).

(G) Estimation of PAR: The PAR sensor on the CTD carousel used the calibration factor determined in 2008 (Hewes, 2008):

$$\mu\text{Eins m}^{-2}\text{ s}^{-1} = 0.0616 \bullet 10^{\text{Volts}}.$$

This PAR sensor was inter-calibrated with the sensor measuring incident PAR in 2008 and determined to have negligible drift between field seasons (Hewes, 2008).

(H) Depth of the euphotic zone (Z_{eu}): Euphotic zone depth is defined as the depth where incident PAR is attenuated to 1% of surface light. Only daytime (08:00 – 24:00 hrs, GMT) stations were used. Transmittance at 5 m was measured by the ratio of incident PAR to PAR measured at the 5 m target depth during bottle firing. A mean (50 stations) transmittance value for 5 m = 34.6 ± 11.4% was obtained. Subsequently, Z_{eu} was de-

Table 2.1. Mean historical values of hydrographic and Chl-*a* data found in each of the areas in the AMLR Survey compared with the 2008/09 field season. The four areas are the Elephant Island Area (EI), Joinville Island Area (JI), South Area (SA), and West Area (WA). The Joinville Island Area had one sample, station A02-13, that was an outlier; this data was removed and corresponding statistics were listed beside JI*.

Area	No. Stations	Temperature, °C	Salinity	Density, kg m^{-3}	Chl-a, mg m^{-3}	Zeu, m	Zuml, m
			Historical AMLR, 1990-2008				
EI	1937	1.36 ± 0.83	34 ± 0.2	27.2 ± 0.2	0.75 ± 0.79	63 ± 40	60 ± 36
JI	83	-0.06 ± 0.96	34.3 ± 0.1	27.5 ± 0.1	0.86 ± 0.53	52 ± 13	110 ± 71
SA	395	1.05 ± 0.88	34.2 ± 0.2	27.4 ± 0.2	1.19 ± 1.06	51 ± 12	56 ± 40
WA	594	1.49 ± 0.64	33.9 ± 0.2	27.2 ± 0.2	0.64 ± 0.68	67 ± 22	52 ± 20
			AMLR, 2009				
EI	48	1.74 ± 0.63	34.1 ± 0.2	27.3 ± 0.2	0.72 ± 0.47	59 ± 17	62 ± 35
JI	11	-0.54 ± 0.16	34.4 ± 0	27.6 ± 0	1.2 ± 0.72	50 ± 6	103 ± 71
SA	20	0.87 ± 1.14	34.3 ± 0.1	27.5 ± 0.1	1.05 ± 0.49	46 ± 12	65 ± 44
WA	23	1.75 ± 0.31	34 ± 0.1	27.2 ± 0.1	0.44 ± 0.48	71 ± 19	43 ± 12
JI*	10	-0.06 ± 0.76	34.3 ± 0.1	27.6 ± 0.1	0.93 ± 0.28	50 ± 6	82 ± 58

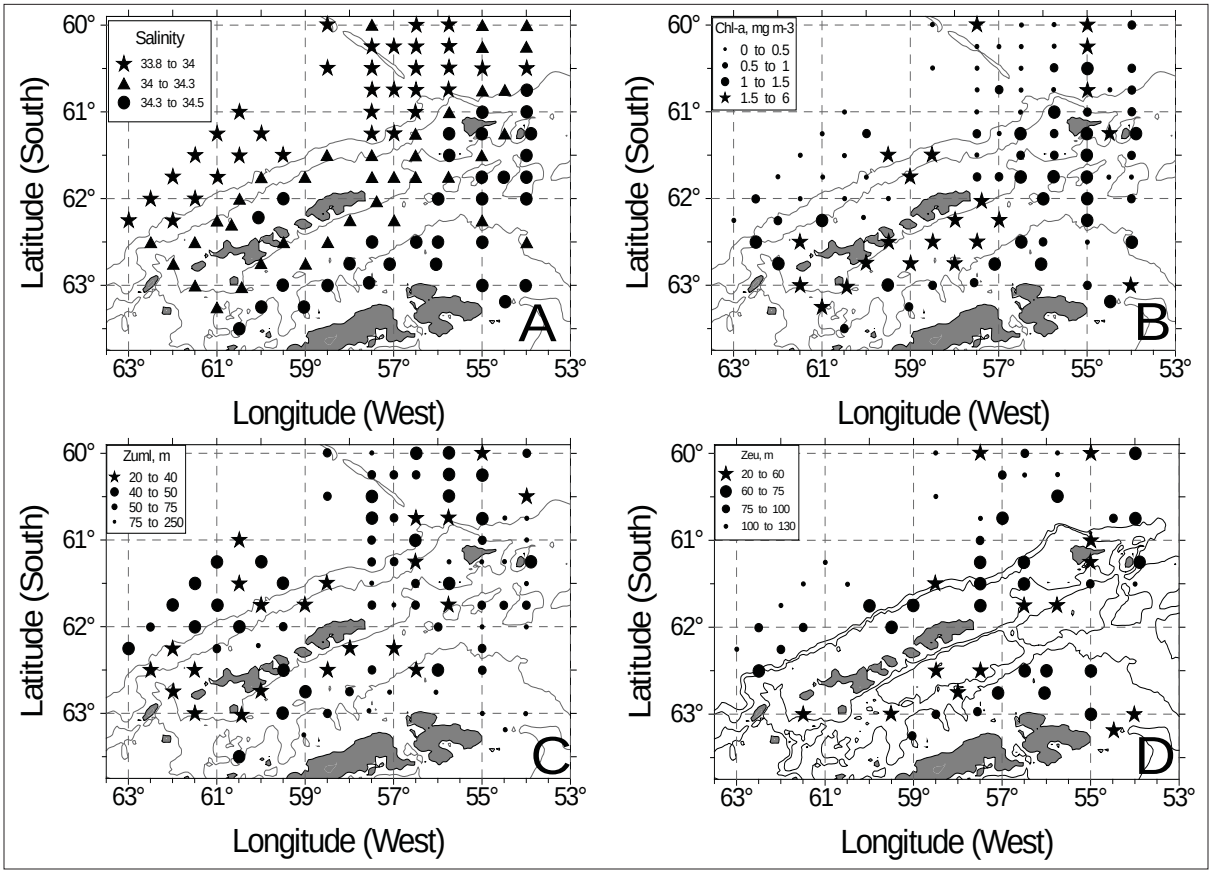

Figure 2.2. Horizontal structure of hydrographic, physical, optical and biological characteristics in the South Shetland Islands: (A) Mean salinity of the UML, grouped into three categories. (B) Surface (5 m target depth) Chl-*a* concentration grouped into four categories. (C) Depth of the UML (meters) grouped into four categories. (D) Depth of the euphotic zone (meters) grouped into four categories; only stations having 5 m PAR > 5 μEin m^{-2} s^{-1} were considered. Contours for 1000 and 2000 m are shown; landmasses are gray.

fined from downcast PAR data as that depth at which:

Transmittance = (PAR at depth) / [(PAR at 5 m) / 34.6)] = 1%.

One percent of incident PAR is defined as measurements having 99.5 – 100.5%, with depth of multiple values within these bounds for a station cast averaged.

(I) Estimation of the mean optical density for incident PAR (OD_{PAR}) in the UML: Optical density is defined as $-\log_{10}$(transmittance), and used here to describe transmittance of incident PAR in the UML. The OD_{PAR} was obtained at those stations where Z_{eu} was measured during the CTD downcast and binned at 1 m intervals. The OD_{PAR} values obtained within the UML were averaged to obtain a mean OD_{PAR}.

(J) Historical data from the South Shetland Islands used in this report are from a database for AMLR Survey data 1990-2007, as reported by Hewes et al. (2009), as well as data from 2008 reported by Hewes et al. (2008b).

Results

A total of 104 phytoplankton samples were collected during the 2008/09 AMLR Survey. The mean Chl-*a* concentrations for the UML in the four areas, together with the long-term mean from previous AMLR seasons (1990-2008), are summarized in Table 2.1. Mean Chl-*a* concentrations in the UML were lowest in the Elephant Island (~0.7 mg m^{-3}) and West (~0.4 mg m^{-3}) Areas, but comparable to the historical mean. Highest mean values were in the Joinville Island Area and the South Area. The Joinville Island Area had a higher mean Chl-*a* value than the historical mean, but station A02-13 was anomalously high (> 5 mg Chl-*a* m^{-3}), whichbiased the mean. Therefore, the Joinville Island Area is listed twice in Table 2.1, showing statistical values with and without station A02-13, as included in the calculations.

The South Shetland Islands can be divided into three biogeochemical regions based on salinity and depth of the UML (Figure 2.2). Using the 2009 data, stations were grouped into three categories of equal intervals, "low", "medium", and "high", according to salinity. Both low- and high-salinity waters generally contain low surface Chl-*a* concentrations, and are considered the two High Nutrient, Low Chlorophyll (HNLC) regions of the South Shetland Islands (Figure 2.2B).

A condition analogous to a "reverse-estuary" is found when high-salinity water from the Weddell Sea flows into the Bransfield Strait to mix with low-salinity Antarctic Surface Water, or AASW. Mid-salinity waters are found encircling the South Shetland Islands and generally contain the highest

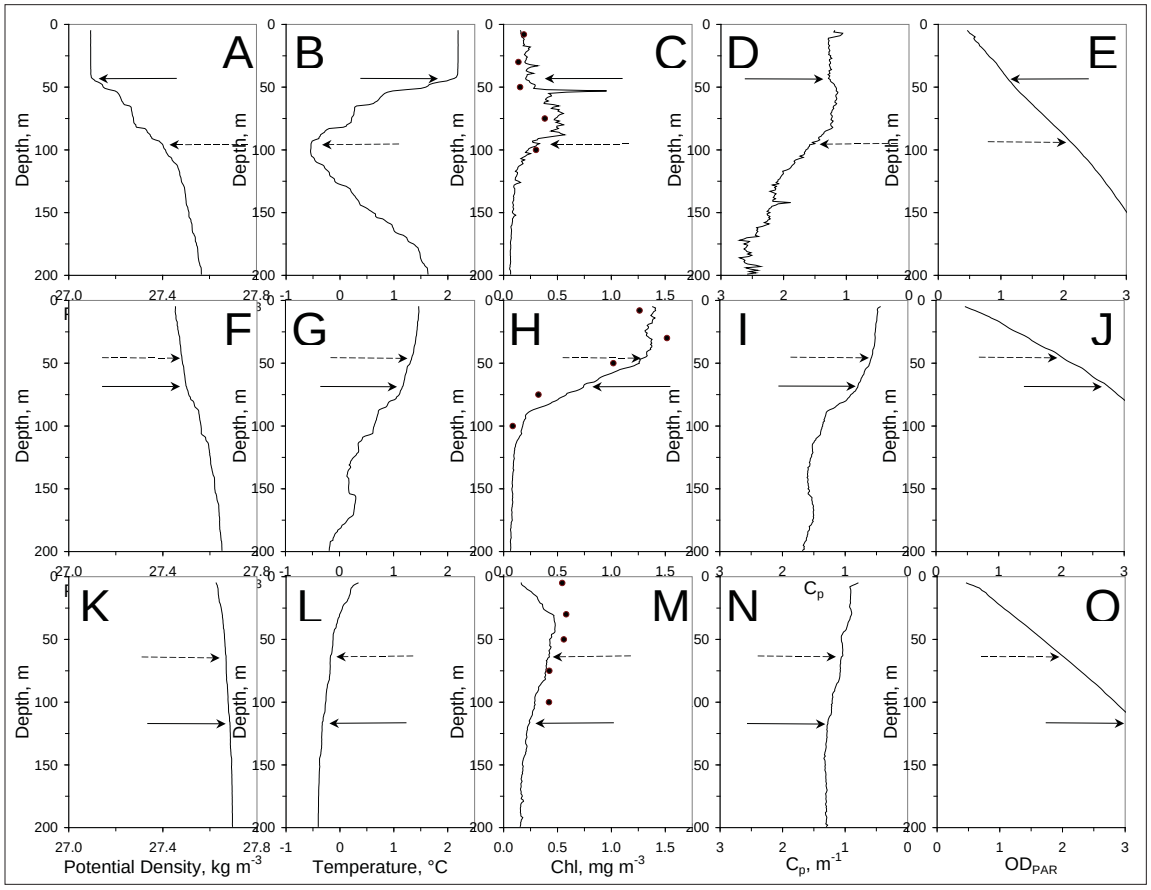

Figure 2.3 Density, temperature, Chl-*a*, beam attenuation, and optical density of incident irradiance in relation to depth for three stations representing different biogeochemical regions observed during Leg I of the AMLR Survey. Station A-0904 (A-E) was of low salinity (mean UML salinity = 33.93), Station A-0408 (F-J) was of intermediate salinity (mean UML salinity = 34.32), and Station A-1214 was of high salinity (mean UML salinity = 34.44). Potential density, temperature, Chl-*a* concentration (as estimated from in situ fluorescence [line] and directly from water bottle sample extracts [filled circles]), beam attenuation and ODPAR are shown for each station. For all stations, depth of the UML (potential density 0.05 kg m^{-3} less than the upper 10 m) is shown as the solid arrow, and depth of the euphotic zone (OD_{PAR} = 2) shown as the dotted arrow.

Chl-*a* concentrations. High-salinity Bransfield Strait waters are associated with deep UML depths, whereas low-salinity Drake Passage waters are associated with relatively shallow UML depths (Figure 2.2C). In turn, low-salinity Drake Passage waters are associated with deep euphotic zones, and contrast with mid-salinity Bransfield Strait waters having shallower Z_{eu} (Figure 2.2D).

Nitrate, phosphate and silicate concentrations at 30 m decrease linearly with the dilution of high-salinity Weddell Sea shelf waters with low-salinity AASW. However, for all waters around the South Shetland Islands, concentrations of these nutrients are well above those considered limiting for phytoplankton biomass.

Three stations, A09-04, A04-08, and A12-14, representing low-, mid-, and high-salinity waters, respectively, are used to illustrate the hydrographic, biological, and optical properties in the upper 200 m of the water column in each biogeochemical region (Figure 2.3).

For low-salinity waters (e.g. station A09-04), the UML is well mixed from the surface to the pycnocline (Figure 2.3A), with warm surface waters overlying cold winter water remnant (Figure 2.3B). Chl-*a* concentrations are uniformly mixed in the UML, as shown by Chl-*a*, Chl_{fluor} (Figure 2.3C), and beam attenuation (Figure 2.3D). Within the pycnocline and above the temperature minimum, there is a deep Chl-*a* maximum. The increased Chl-*a* concentration in the deep Chl-*a* maximum attenuates more incident irradiance than the UML, indicated by the inflection for OD_{PAR} (Figure 2.3E)

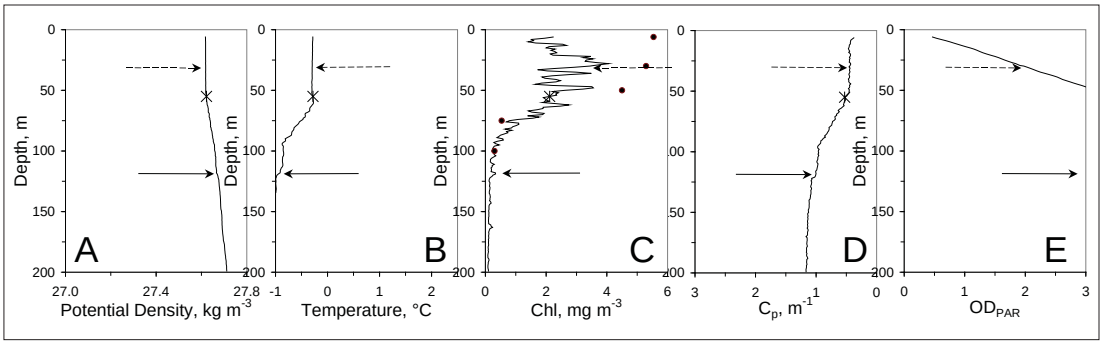

Figure 2.4. Anomalous Station A02-13: Potential density, temperature, Chl-*a* concentration (as estimated from in situ fluorescence [line] and directly from water bottle sample extracts [filled circles]), beam attenuation and ODPAR are shown. Depth of the UML (potential density 0.05 kg m-3 less than the upper 10 m) shown as the solid arrow, and depth of the euphotic zone (ODPAR = 2) shown as the dotted arrow. Note the scaling for Chl-*a* in C is different than used in Fig. 2.3. The beginning of the thermocline at 55 m is indicated by X.

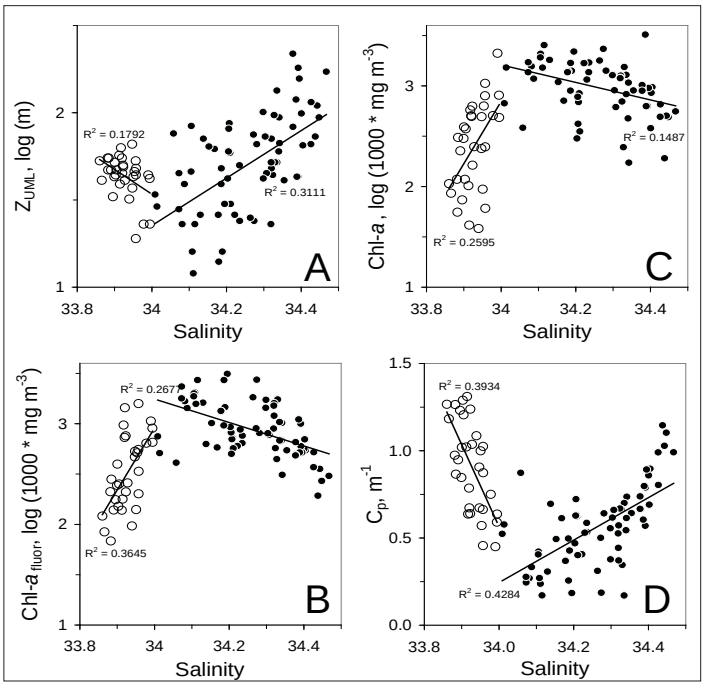

Figure 2.5. Proxies of phytoplankton biomass as functions of UML depth. (A) Log mean Chl-*a* concentration of the UML, (B) mean transmittance of the UML, and (C) log mean Chl_{fluor} of the UML were significantly ($p < 0.01$) correlated with UML depth for salinities >34 (solid symbols) but not correlated for salinities <34. However, all proxies of phytoplankton biomass were significantly lower (ANOVA, $p < 0.01$) for low-salinity waters in relation to their Z_{UML}.

between the UML and euphotic zone depths. In addition, the 1% value of incident irradience ($OD_{PAR} = 2$) corresponded with the base of the deep Chl-*a* maximum (Figure 2.3C, D). Furthermore, the depth at 1% incident irradiance (Figure 2.3E) extended much deeper than the depth of the UML (Figure 2.3A).

For mid-salinity waters (e.g. station A04-08), the difference in potential density between the surface and depth (Figure 2.3F) was less pronounced than for low-salinity waters. UML temperatures are lower (Figure 2.3G), and Chl-*a* (Figure 2.3H) and beam attenuation (Figure 2.3I) decline slightly between the depth of 1% incident irradiance and UML depth, which is reflected in a slight bend in the attenuation of incident irradiance at depth (Figure 2.3J). Station A04-08 contained ~5 times more Chl-*a* in the UML than Station A09-04 (Figure 2.3C, H), which resulted in greater attenuation of incident irradiance at depth (Figure 2.3E, J) and reduced depth of the euphotic zone by ~50%.

For high-salinity waters (e.g. station A12-14), the water column was weakly stratified (Figure 2.3K), associated with a deep UML. However, water temperature was not vertically uniform (Figure 2.3L), indicative of weak stratification. Both Chl-*a* (Figure 2.3M; photoinhibition of Chl-*a* fluorescence occurred in the upper 30 m) and beam attenuation (Figure 2.3N) also indicate that mixing in the UML was not uniform.

Station A02-13 was of high-salinity, deeply mixed water, and yet had the highest Chl-*a* concentration measured during the AMLR Survey (Figure 2.4). In contrast to either Stations A04-08 or A12-14, Station A02-13 had a very uniform UML from the surface to 55 m (Figure 2.4A), as evidenced by temperature (Figure 2.4B). Below 55 m, temperature gently eroded to about -1 °C at ~125 m that was considered the bottom of the UML (i.e., 0.05 kg m^{-3} difference from the surface).

For high- to mid-salinity waters, ln Chl-*a* (Figure 2.5C) and ln Chl_{fluor} (Figure 2.5B) are negatively correlated with UML depth ($p < 0.01$). No significant correlation was found in low-salinity waters, although Chl-*a* and Chl_{fluor} values were lower, and C_p values higher (ANOVA, $p < 0.01$) than found in higher salinity waters with the same Z_{UML}.

Historical comparison

For low-salinity water, Z_{UML} was deep compared to the historical (1990-2007) mean, while mid-salinity waters had shallower Z_{UML} than the historical mean (Figure 2.6A). Mean Chl-*a* of the UML in low-salinity waters was lower than the historical mean, while both mid- and high-salinity waters were slightly above the historical mean (Figure 2.6B). The data from the 2009 AMLR Survey were similar to those of the 2008 AMLR Survey with respect to both Z_{UML} and mean Chl-*a* of the UML (Figure 2.6).

Discussion

In 2009 (as well as 2008; see Hewes et al., 2008b), Chl-*a* concentrations were lower than average and UML depths were deeper than the historical average, suggesting that light and iron both controlled phytoplankton biomass in low-salinity waters. There is evidence that low light conditions increase the iron demand of phytoplankton for synthesis of

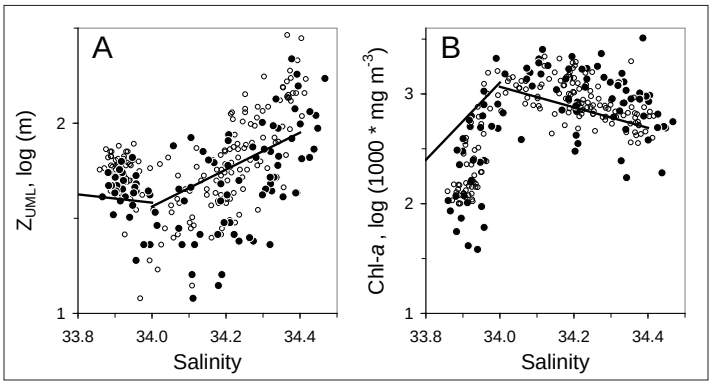

Figure 2.6. Comparison of 2009 Chl-*a* concentration and UML depth with historical data. Unimodal distributions of (A) Depth of the UML, and (B) mean UML Chl-*a* concentration in relation to salinity for 2009 (filled symbols) compared with 2008 data (open symbols). Lines drawn are for the historical (1990, 1992-1994, 1996-2007) means; 1991 and 1995 were anomalous years, therefore excluded. Both 2008 and 2009 had deeper UML depths and lower mean UML Chl-*a* concentrations at low-salinities than the 16-year mean, while both 2008 and 2009 had shallower UML depths and higher mean UML Chl-*a* concentrations than the 16-year mean.

proteins in photoreceptors (Sunda and Huntsman, 1997; Strzepek and Harrison, 2004), and an iron/light co-limitation could be an explanation for the lower Chl-*a* concentration found corresponding with deeper Z_{UML} in the presumably iron-controlled HNLC area of the Drake Passage.

The mean Chl-*a* concentration of the UML for mid-salinity waters measured during the 2008/09 AMLR Survey was higher than the 1990-2007 mean. Temperature of the UML in both the South Area and the Elephant Island Area was warmer than average.

Lastly, stations A02-13 and A03-14, near Joinville Island, were anomalous, having deeply mixed UMLs and Chl-*a* concentrations >1 mg m^{-3}. UML depth is defined as the depth at which there is a 0.05 kg m^{-3} difference from surface pressure; the UML depth at station A02-13 is 125 m. However, there was a broad thermocline beginning at 55 m, with a uniform UML above 55 m and decreasing Chl-*a* below 55 m. Therefore, the operational definition of UML, using the 0.05 mg m^{-3} difference from surface density, may be too large a value under certain hydrographic conditions.

CTD casts have been completed at 80 stations in the Joinville Island Area since 1990, approximately 40 of these completed south of 62.25°S. Of these, 10 stations had UML depths >75 m and Chl-*a* concentrations >0.5 mg m^{-3}; four stations had >1 mg Chl-*a* m^{-3}. With so few data, however, it is speculative to assign causes for these anomalies, although such exceptions are curious and worthy of further investigation.

Protocol Deviations

Chl-*a* measurements were restricted to bottle sample depths of 5, 10, 30, 50, 75, and 100 m for this survey period. Samples for phytoplankton taxonomy are in the process of being analyzed at the time of this report.

Disposition of the Data

Data are available from Christian S. Reiss, NOAA Fisheries, Antarctic Ecosystem Research Division, 3333 Torrey Pines Court, Room 412, La Jolla, CA 92037. Ph: 858-546-7127, FAX: 858-546-5608

Acknowledgements

We want to express our gratitude and appreciation to the entire complement of the R/V *Yuzhmorgeologiya* for their generous and valuable help during the entire cruise. They not only aided immeasurably in our ability to obtain the desired oceanographic data, but they also made the cruise most enjoyable and rewarding in many ways. We also thank all other AMLR personnel for help and support that was essential to the success of our program. This report has been funded in part to O. Holm-Hansen from the National Oceanic and Atmospheric Administration, U.S. Department of Commerce, under grant NA17RJ1231. The views expressed herein are those of the authors and do not necessarily reflect the views of NOAA, NSF, NASA or any of their sub-agencies.

References

Hewes, C.D. 2008. Calibration of the US AMLR Program's Photosynthetically Available Radiation (PAR) sensors. In: Van Cise, A.M., (ed.) AMLR 2007/2008 Field Season Report. NOAA-TM-NMFS-SWFSC-427. NMFS Southwest Fisheries Science Center, La Jolla, CA.

Hewes, C.D., C.S. Reiss, M. Kahru, B.G. Mitchell, O. Holm-Hansen, 2008a. Control of phytoplankton biomass by dilution and mixing depth in the western Weddell-Scotia Confluence. Marine Ecology Progress Series, 366: 15-29.

Hewes, C.D., B. Seegers, H. Wang, M. Kahru, B.G. Mitchell, O. Holm-Hansen, M.V. Ardelan, K.C. Bizsel, M.J. Calderón Nash, N.V. Santana Viviana, J.L. Iriarte, N. Silva and C. Carrasco. 2008b. Phytoplankton Studies in the South Shetland Islands and South Orkney Islands Area. In: Lipsky, J.D. (ed.) AMLR 2007/2008 Field Season Report. NOAA-TM-NMFS-SWFSC-427. NMFS Southwest Fisheries Science Center, La Jolla, CA.

Hewes, C.D., C.S. Reiss, O. Holm-Hansen, 2009. A quantitative analysis of sources for summertime phytoplankton variability over 18 years in the South Shetland Islands (Antarctica) region. Deep-Sea Research I, in press.

Holm-Hansen, O., C. J. Lorenzen, R. W. Holmes and J. D. H. Strickland. 1965. Fluorometric determination of chlorophyll. J. Cons. perm. int. Explor. Mer 30: 3-15.

Holm-Hansen, O. and B. Riemann. 1978. Chlorophyll a determination: Improvements.in methodology. OIKOS 30: 438-447.

Needham, D. 2009. Physical Oceanography and Underway Environmental Observations. Pp. 2-6 In: Van Cise, A.M. (ed.) AMLR 2008/2009 Field Season Report. NOAA-TM-NMFS-SWFSC-445. NMFS Southwest Fisheries Science Center, La Jolla, CA.

Strzepek, R.F., and P.J. Harrison. 2004. Photosynthetic architecture differs in coastal and oceanic diatoms. Nature 431: 689-692.

Sunda, W.G., and S.A. Huntsman. 1997. Interrelated influence of iron, light and cell size on marine phytoplankton growth. Nature 390: 389-392.

Villafañe, V., E. W. Helbling and O. Holm-Hansen. 1993. Phytoplankton around Elephant Island, Antarctica: distribution, biomass and composition. Polar Biology 13: 183-191.

UNITED STATES
AMLR ANTARCTIC MARINE LIVING RESOURCES PROGRAM

AMLR 2008/2009 FIELD SEASON REPORT

Objectives, Accomplishments and Tentative Conclusions

Edited by
Amy M. Van Cise

May 2009

NOAA-TM-NMFS-SWFSC-445

U.S Department of Commerce
National Oceanic & Atmospheric Administration
National Marine Fisheries Service
Southwest Fisheries Science Center
Antarctic Ecosystem Research Division
8604 La Jolla Shores Drive
La Jolla, California, U.S.A. 92037

The National Oceanic and Atmospheric Administration (NOAA), organized in 1970, has evolved into an agency which establishes national policies and manages and conserves our oceanic, coastal, and atmospheric resources. An organizational element within NOAA, the Office of Fisheries is responsible for fisheries policy and the direction of the National Marine Fisheries Service (NMFS).

In addition to its formal publications, the NMFS uses the NOAA Technical Memorandum series to issue informal scientific and technical publications when complete formal review and editorial processing are not appropriate or feasible. Documents within this series, however, reflect sound professional work and may be referenced in the formal scientific and technical literature.

The U.S. Antarctic Marine Living Resources (AMLR) program provides information needed to formulate U.S. policy on the conservation and international management of resources living in the oceans surrounding Antarctica. The program advises the U.S. delegation to the Convention for the Conservation of Antarctic Marine Living Resources (CCAMLR), part of the Antarctic treaty system. The U.S. AMLR program is managed by the Antarctic Ecosystem Research Group located at the Southwest Fisheries Science Center in La Jolla.

Inquiries should be addressed to:

Antarctic Ecosystem Research Group
Southwest Fisheries Science Center
8604 La Jolla Shores Drive
La Jolla, California, USA 92037

Telephone Number: (858) 546-5600
E-mail: Amy.VanCise@noaa.gov